EURODYN 2020
XI International Conference on Structural Dynamics
M. Papadrakakis, M. Fragiadakis, C. Papadimitriou (eds.)
Athens, Greece, 23–26 November 2020

FE MODEL UPDATING OF MASONRY TOWERS: MODELING AND NUMERICAL ISSUES

R.M. Azzara[1], M. Girardi[2], C. Padovani[2], D. Pellegrini[2], and L. Robol[3,2]

[1]Istituto Nazionale di Geofisica e Vulcanologia (INGV), Osservatorio Sismologico di Arezzo
Via Francesco Redi, 13, 52100, Arezzo, Italy
riccardo.azzara@ingv.it

[2]Institute of Information Science and Technologies "A. Faedo"
Via G. Moruzzi, 1, 56124 Pisa, Italy
{maria.girardi, cristina.padovani, daniele.pellegrini}@isti.cnr.it

[3] Department of Mathematics, University of Pisa
Largo B. Pontecorvo, 5, 56127, Pisa, Italy
leonardo.robol@unipi.it

Keywords: Dynamic monitoring, soil-structure analysis, model updating

Abstract. *The goal of this paper is to investigate the role of soil-structure interaction in modeling the dynamic behavior of masonry towers. The study, conducted on the bell tower of the Basilica of San Frediano in Lucca (Italy), is based on both experimental and numerical results. The former were collected during an experimental campaign carried out on the tower using seismometric stations, while the latter have been obtained via the modal analysis and model updating procedures implemented in the finite element code NOSA-ITACA. Combining experimental and numerical outcomes made it possible to assess the influence of the soil, modeled as a system of elastic springs, on the natural frequencies of the tower. Finite element models of the tower have been calibrated by taking the presence of the adjacent church into account and choosing different unknown parameters, including the soil stiffness.*

1 INTRODUCTION

Finite element (FE) model updating techniques are based on solution of a constrained minimum problem, in which the objective function is generally expressed as the discrepancy between experimental and numerical natural frequencies and mode shapes [1]. Wide application of these techniques to heritage structures is quite recent [2], [3], [4].

An efficient algorithm for model updating based on a modified Lanczos projection strategy and a trust-region scheme has been implemented in NOSA-ITACA, free software developed in house by ISTI-CNR and successfully applied to several case studies [5, 6]. Besides reducing the overall computation time of the numerical process and enabling accurate analysis of large-scale models with little effort, the proposed algorithm allows for obtaining information on both the reliability of the solution and its sensitivity to noisy experimental data.

Recent studies have shown that soil-structure interaction should be taken into account in studying the dynamic behavior of masonry structures [7], [8], [9], [10], [11], [12]. Stemming from the results of a continuous monitoring campaign conducted by the authors on the San Frediano belfry in the historic center of Lucca [13], this paper is aimed at investigating how this interaction influences the results of model updating.

In [13] FE model updating of the tower was conducted, by taking the presence of the adjacent church into account via suitable boundary conditions and considering the tower clamped at the base. In the present paper, the soil-structure interaction is studied by applying at the structure's base a system of elastic springs whose stiffness is varied in order to represent different soil types [14]. Two models of the tower have been analyzed: in the former the tower is free, and the influence of the church neglected, while in the latter the presence of the lateral walls of the church is modelled via elastic springs. The influence of soil stiffness on the tower's natural frequencies has been investigated and the model updating procedure implemented in NOSA-ITACA [5], [6] has been applied to determine the optimal mechanical properties of the tower-springs system.

2 FE MODEL UPDATING

Numerical modeling of a structure is usually characterized by several uncertainties regarding the properties of the constituent materials, the constraining effect of the adjacent buildings, boundary conditions, local soil conditions, etc. Model updating is a procedure aimed at determining some unknown parameters of a FE model in order to match the experimental and numerical dynamic properties of a structure (frequencies and mode shapes) [1]. Assuming that the stiffness and mass matrices of a structure discretized into finite elements depends on a parameter vector x varying in a p-dimensional box Ω, we want to determine the optimal value of x that minimizes, within the box Ω, the objective function

$$\phi(\mathrm{x}) = \sum_{i=1}^{q} w_i^2 [f_i^{exp} - f_i(\mathrm{x})]^2, \tag{1}$$

where f_i^{exp} and $f_i(\mathrm{x})$ are the q experimental and numerical frequencies to match (with q not less than p). In particular, numerical frequencies $f_i(\mathrm{x})$ are calculated by solving a generalized eigenvalue problem involving the stiffness matrix K(x) and mass matrix M(x) depending on the parameter vector x. Scalars w_i are the weight that should be given to each frequency in the optimization scheme; in order to obtain satisfactory accuracy on the frequencies, w_i is usually chosen as equal to the inverse of the experimental frequency.

The numerical procedure for model updating, described in detail in [5, 6], has been implemented in the NOSA-ITACA code, a finite element software package developed in house by

ISTI-CNR [15], for performing modal analyses [16] and managing the large-scale problems encountered in applications.

The algorithm implemented in the code is based on construction of local parametric reduced-order models embedded in a trust-region scheme for solving the constrained minimum problem. In particular, the algorithm exploits the structure of the stiffness and mass matrices and the fact that only a few of the smallest eigenvalues have to be calculated in order to solve the problem.

3 THE SAN FREDIANO BELL TOWER

The bell tower of the Basilica of San Frediano (Figure 1), dating back to the 11th century, is one of the best preserved in Lucca's historic center. The tower, whose geometry is sketched in Figure 2 and described thoroughly in [13], is 52 m high, with walls varying in thickness from about 2.1 m at the base to 1.6 m at the top. The San Frediano Basilica adjoins the tower on two sides for about 13 m of its height. The masonry constituting the tower appears to be made of regular stone blocks at the base, while quite homogeneous brick masonry is visible in the upper sections, apart from the central part of the walls, where the masonry between the windows is made up of stone blocks.

In the period 2015-2017 the tower was instrumented with four SARA tri-axial seismometric stations, each made up of a SL06 24-bit digitizer and a SS20 seismometer (electrodynamic velocity transducer, 2.0 Hz eigenfrequency), made available by the Arezzo Seismology Observatory (INGV). The instruments were arranged on the San Frediano bell tower adopting different sensors layouts and data recorded were analyzed via the Covariance Driven Stochastic Subspace Identification method (SSI/Cov) [17], [18] implemented in the MACEC code [19].

Table 1 reports the mean values of the first five frequencies calculated using data recorded in August 2016, with a sampling frequency of 100 Hz. The first and second frequencies correspond to flexural mode shapes along the X and Y direction, respectively. The third frequency is likely related to a torsional mode shape. The last two frequencies correspond once again to flexural model shapes. More details on mode shapes are given in [13].

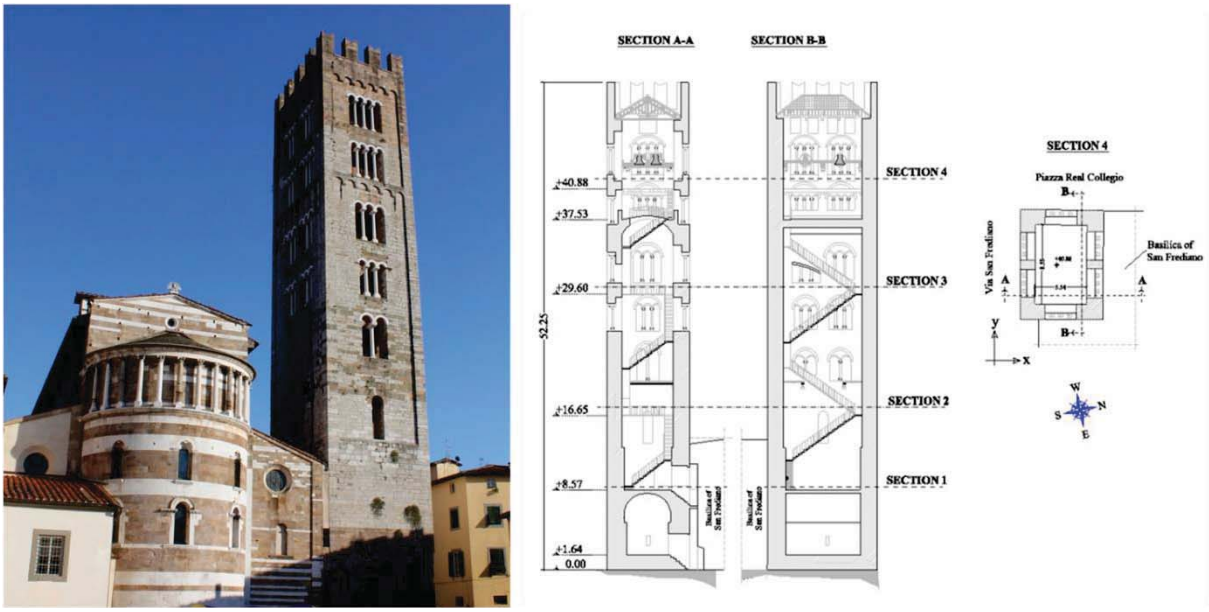

Figure 1: The San Frediano bell tower.

	Frequency [Hz]
Mode 1 (Bending X)	1.11
Mode 2 (Bending Y)	1.39
Mode 3 (Torsional)	3.45
Mode 4 (Bending X)	4.64
Mode 5 (Bending Y)	5.37

Table 1: The first five frequencies of the San Frediano bell tower.

3.1 FE modeling, modal analysis and model updating

This section is devoted to the modal analysis of the bell tower. All numerical analyses presented in this paper have been conducted via the NOSA–ITACA code [5], [6], [16], [15].
The San Frediano bell tower has been discretized into 45935 brick and 673 beam and truss elements (element n. 8, 9 and 35 in [15]) with 60228 nodes, as shown in Figure 2. Beams have been used to model the steel tie rods and the wooden roof elements, while trusses are used for the springs at the base, according to the Winkler model for the soil [14] and to model the adjacent building. In particular, two models have been considered: in the former (Model 1) the presence of the church is neglected, while in the latter (Model 2) elastic spring have been applied 12.50 m above the base to account for the church's adjacent walls (red springs along X and magenta springs along Y in Figure 2). In both cases horizontal displacements of the base are prevented and vertical displacement is constrained by the presence of elastic springs under the tower's base (green in Figure 2).
The masonry has been modeled as an isotropic linear elastic material with Poisson's ratio $\nu = 0.2$, mass density $\rho = 2000$ kg/m^3, and Young's modulus E_m varying from 2.0 GPa to 10.0 GPa. Figures 3 to 7 show the first five frequencies of Model 1 as functions of E_m, with the soil stiffness k_w taking values between 4800 and 128000 kN/m^3, corresponding respectively to loose and dense sand [14]. As expected, for fixed k_w, the frequencies are increasing functions of Young's modulus. The first and second frequencies remain strictly below the corresponding experimental frequencies, likely due to the fact that the real system is considerably stiffer than its numerical model. For fixed E_m, the frequencies increase as soil stiffness k_w increases, but this rise becomes less evident as Young's modulus increases; for example, the first frequency increases by about 44% when E_m=2 GPa and k_w ranges from 4800 kN/m^3 to 128000 kN/m^3, while for E_m=10 GPa the growth of the first frequency is on the order of 18.5%. Furthermore, there is visibly greater influence of the soil stiffness on the two first bending frequencies than on higher-order ones. With respect to the experimental mode shapes, the MAC values [18] are consistently greater than 0.9, and their variation with soil stiffness is not appreciable.

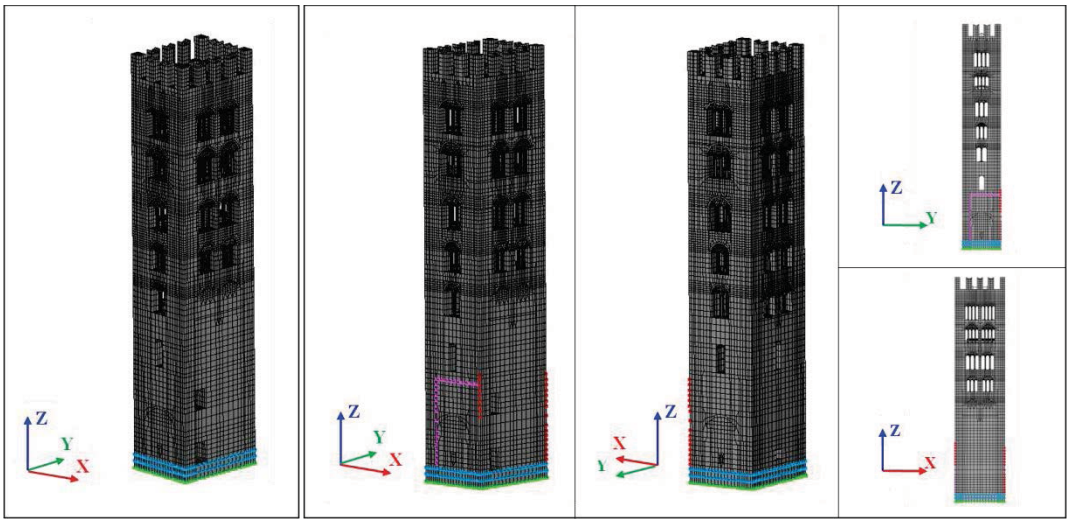

Figure 2: FE discretization of the San Frediano bell tower, model 1 (left) and model 2 (right). In model 1 and model 2 the soil is modeled as vertical springs (green) and the displacements along X and Y are prevented at the base (cyan). In model 2 the presence of the adjacent church is modeled as springs along X (red) and Y (magenta).

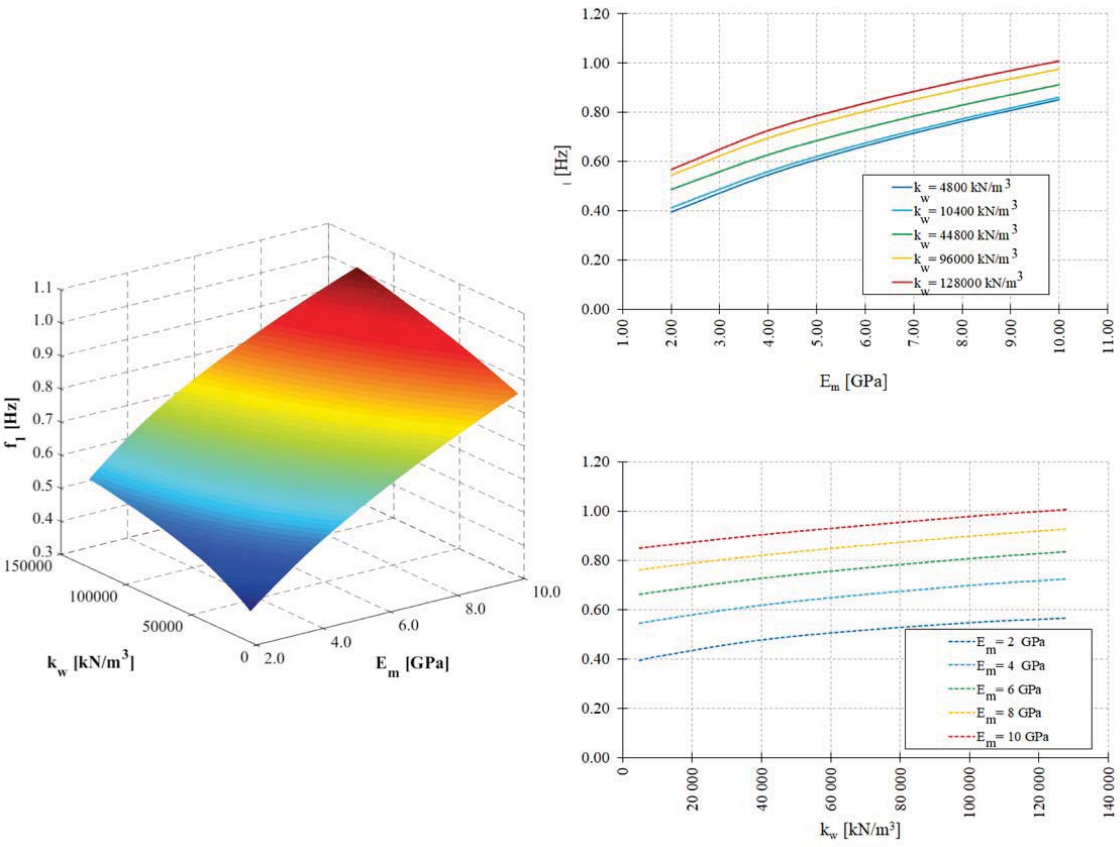

Figure 3: Model 1, first frequency as a function of Young's modulus E_m and soil stiffness k_w.

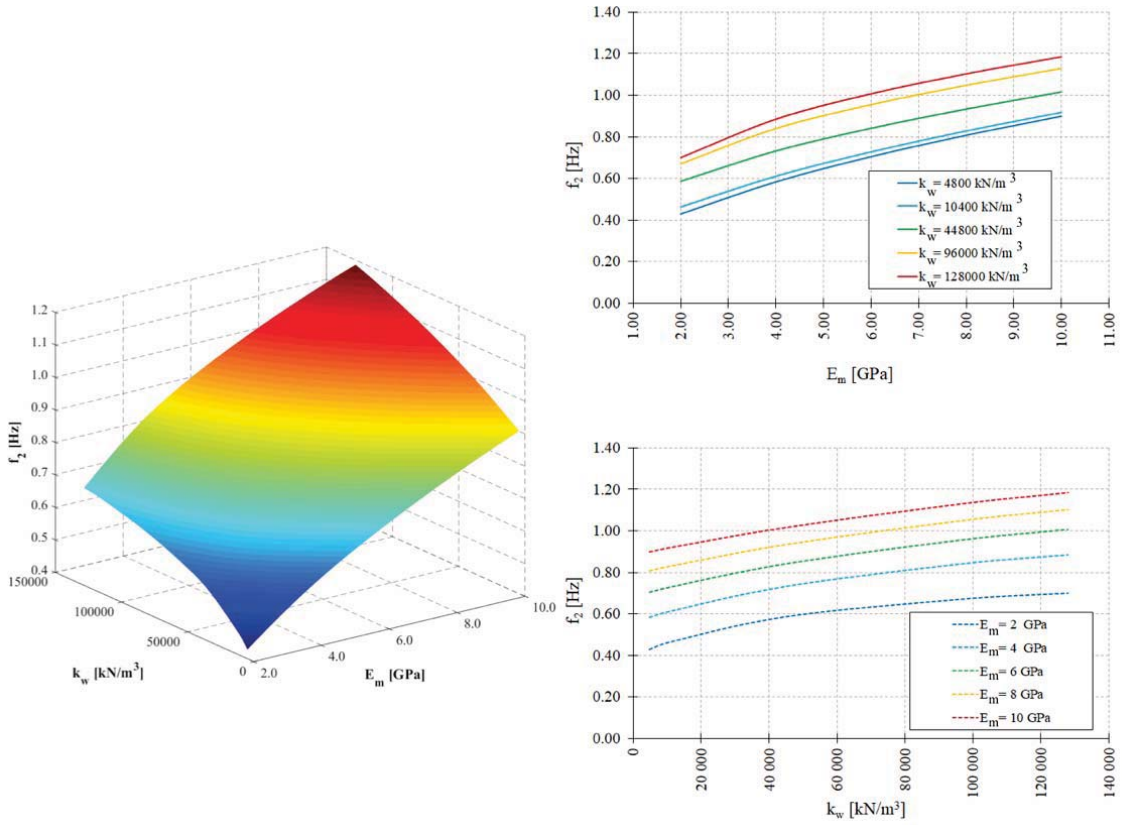

Figure 4: Model 1, second frequency as a function of Young's modulus E_m and soil stiffness k_w.

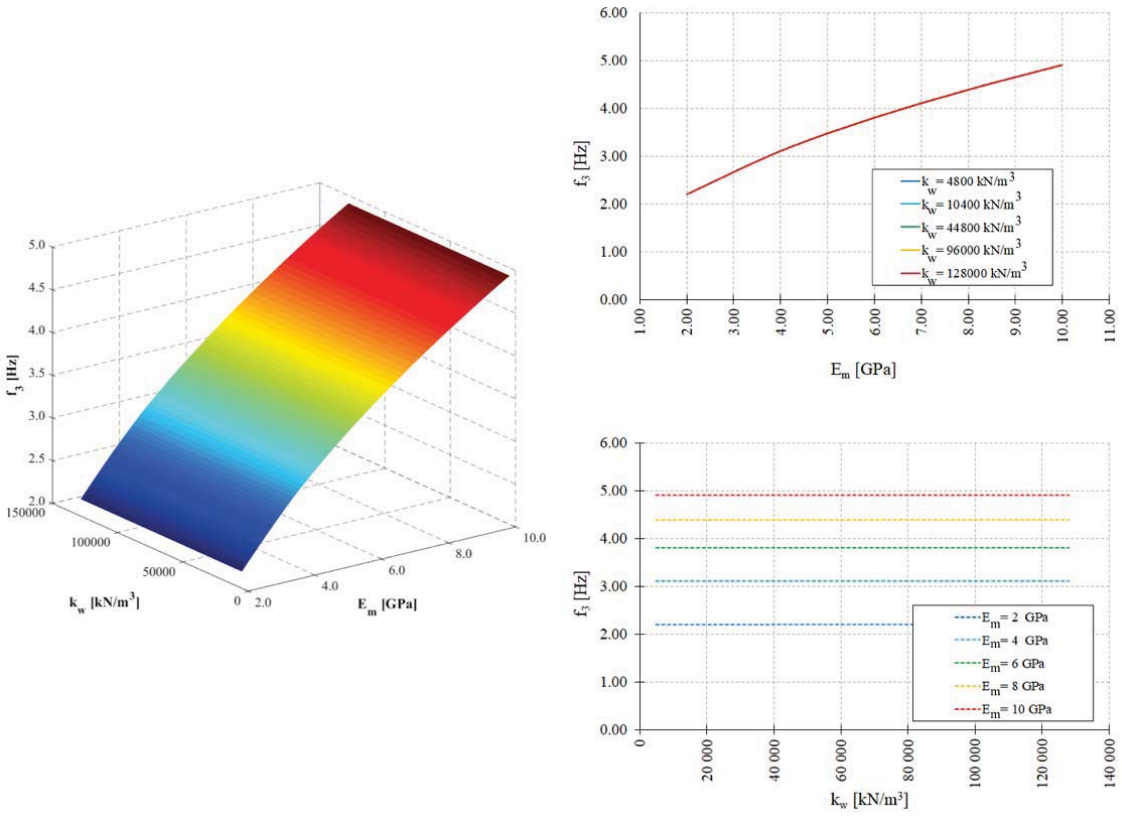

Figure 5: Model 1, third frequency as a function of Young's modulus E_m and soil stiffness k_w.

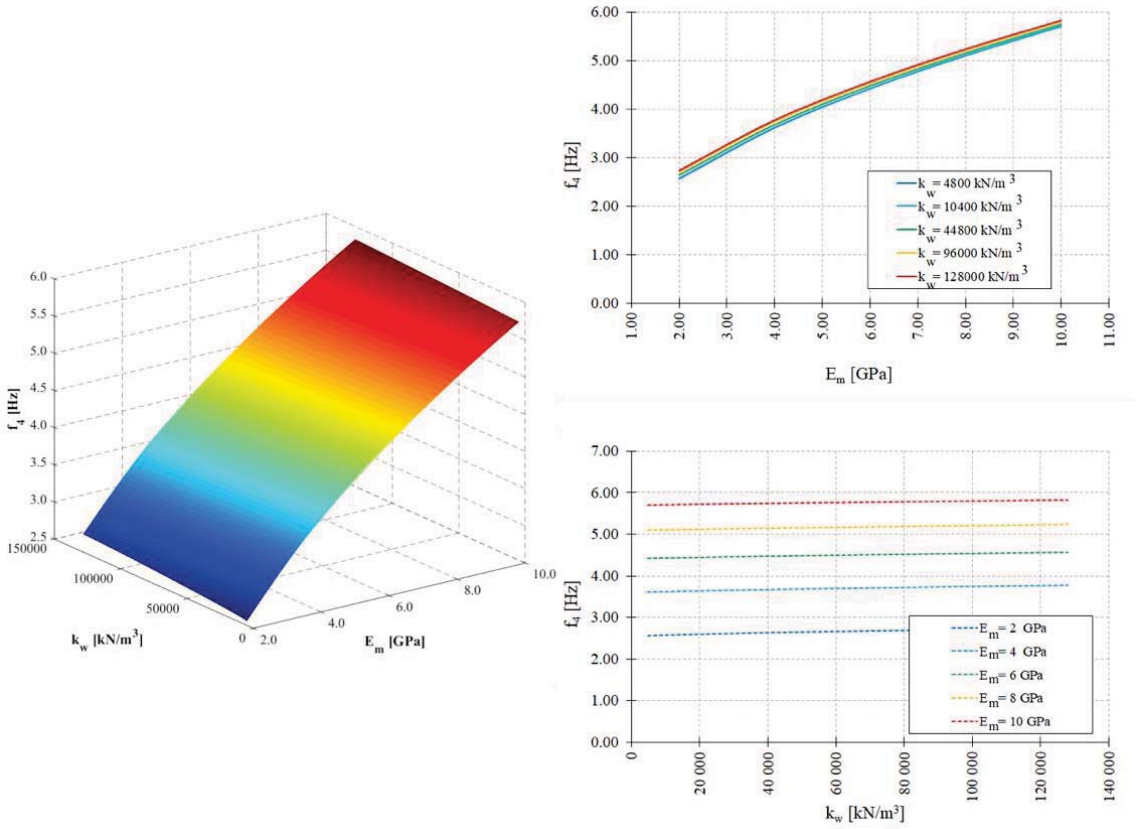

Figure 6: Model 1, fourth frequency as a function of Young's modulus E_m and soil stiffness k_w.

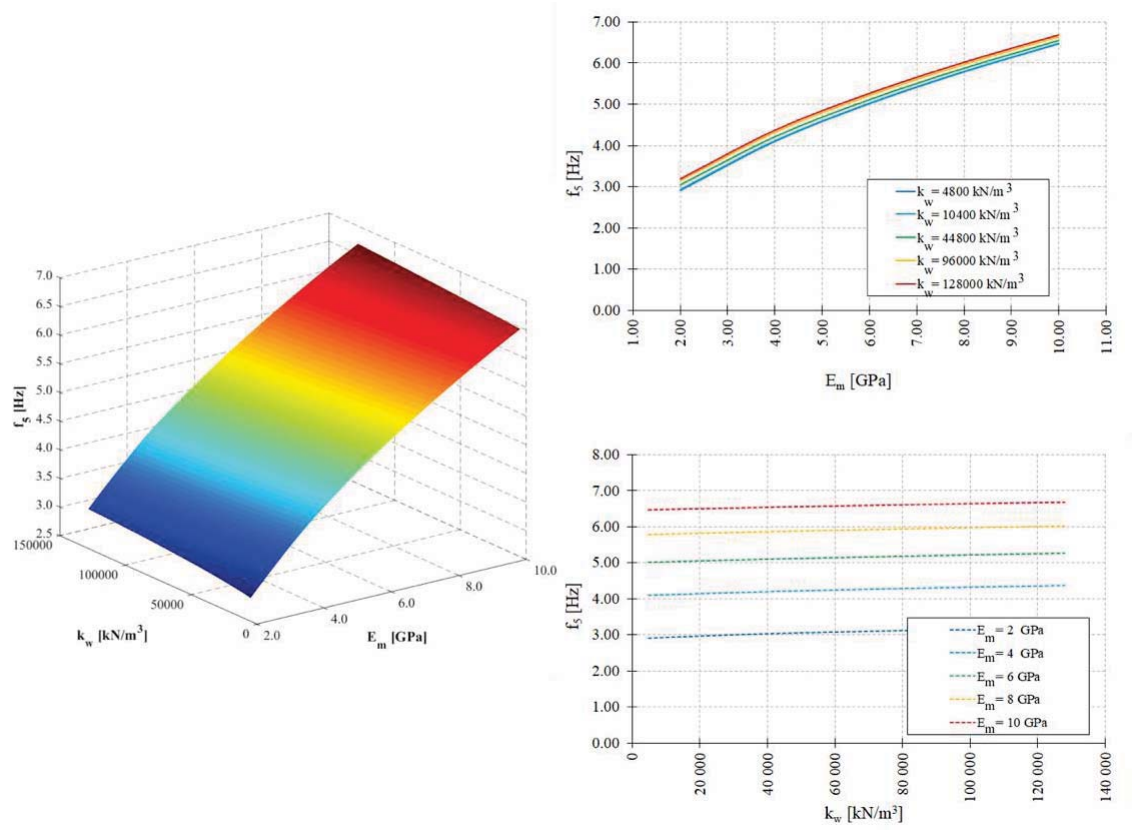

Figure 7: Model 1, fifth frequency as a function of Young's modulus E_m and soil stiffness k_w.

The model updating procedure described in [5] and [6] is conducted on Model 1 considering the unknown parameters masonry's Young's modulus E_m [GPa] and the soil stiffness k_w [kN/m^3] ranging in the intervals

$$E_m \in [1.0, 10.0] \text{ GPa}, \qquad k_w \in [4800.0, 128000.0] \text{ kN/m}^3. \tag{2}$$

The procedure provides the following values

$$E_m^{opt} = 6.61 \text{ GPa}, \quad k_w^{opt} = 1.28\ 10^5 \text{ kN/m}^3, \tag{3}$$

with k_w^{opt} coinciding with the right end of the interval in (2). The corresponding numerical frequencies and the relative errors with respect to the experimental frequencies are summarized in Table 2.

	Exp. freq. [Hz]	Num. freq. [Hz]	Relative error [%]
Mode 1	1.11	0.87	21.62
Mode 2	1.39	1.04	25.18
Mode 3	3.45	3.99	-15.65
Mode 4	4.64	4.78	-3.02
Mode 5	5.37	5.51	-2.61

Table 2: The first five numerical frequencies of Model 1 corresponding to the optimal values in (3) with the relative errors with respect to the experimental values.

The errors shown in the Table demonstrate that Model 1 is not able to capture the dynamic response of the real system.

Model 2 differs from Model 1 in that elastic springs are now applied 12.50 m above the base to account for the adjacent church walls. Let us fix the elastic constants of the springs: k_X = 7.75 10^7 N/m for the springs along X (red in Figure 2) and k_Y = 1.5 10^8 N/m for the springs along Y (magenta in Figure 2). These constants have been determined by considering the presence of the adjacent church, whose walls have a shear stiffness of about 2.4 10^9 N/m in the Y direction and 1.89 10^9 N/m in the X direction. As for the church's constituent material, a shear modulus of 1.25 GPa and a Poisson's ratio of 0.2 have been assumed [20].

Figures 8 to 12 show the first five frequencies of Model 2 as functions of E_m and soil stiffness k_w. Dashed lines represent the experimental frequency values.

As in Model 1, for fixed k_w, the frequencies are increasing functions of Young's modulus and for fixed E_m the frequencies increase with increasing soil stiffness k_w. However, in this case the growth is more or less steady; for example, the first frequency increases by about 6.45% when E_m=2 GPa and the value of k_w is increased from e 4800 kN/m^3 to 128000 kN/m^3, while for E_m=10 GPa the corresponding increase is about of 5.84%.

In this case, unlike in Model 1, the five frequencies of the tower are less influenced by soil stiffness. In fact, the tower's bending stiffness is mainly influenced by the constraint of the adjacent walls, while the vertical deformability of the soil under the base seems to make a negligible contribution to the overall deformability of the system. In this case, also unlike in Model 1, the experimental frequency values intercept the surfaces of the numerical frequencies, thus indicating that Model 2 can provide a good approximation of the actual dynamic behavior of the tower.

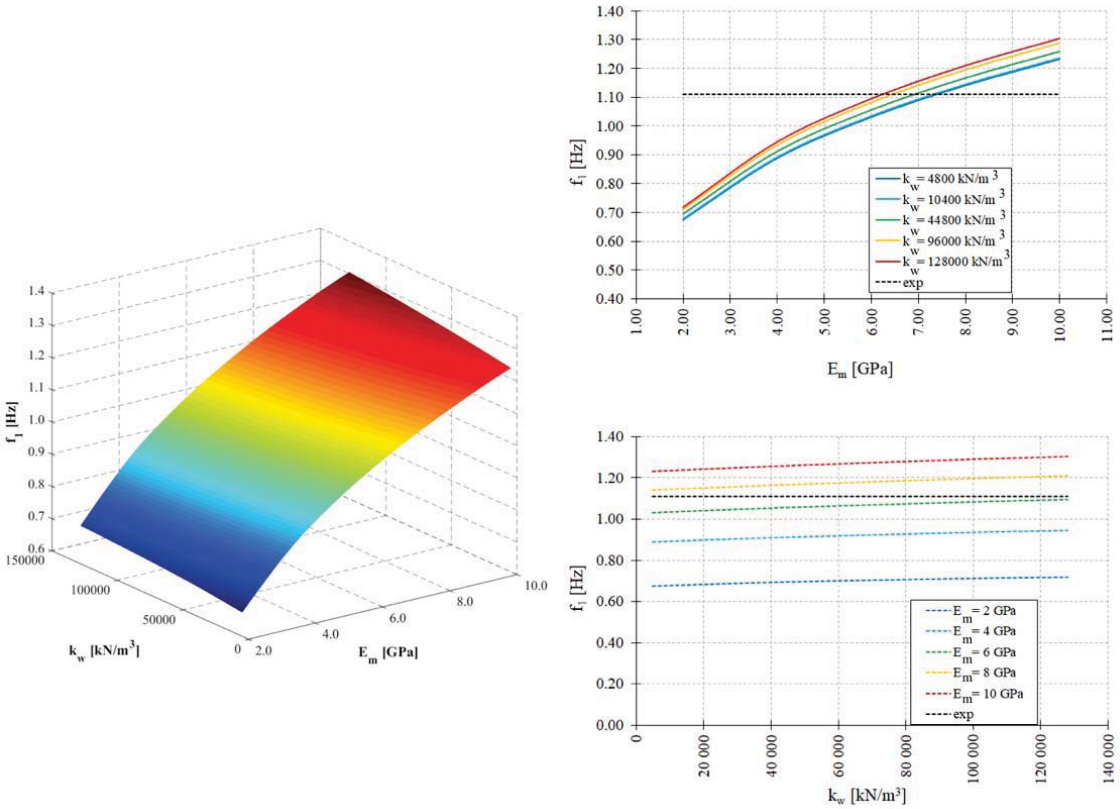

Figure 8: Model 2, first frequency as a function of Young's modulus E_m and soil stiffness k_w.

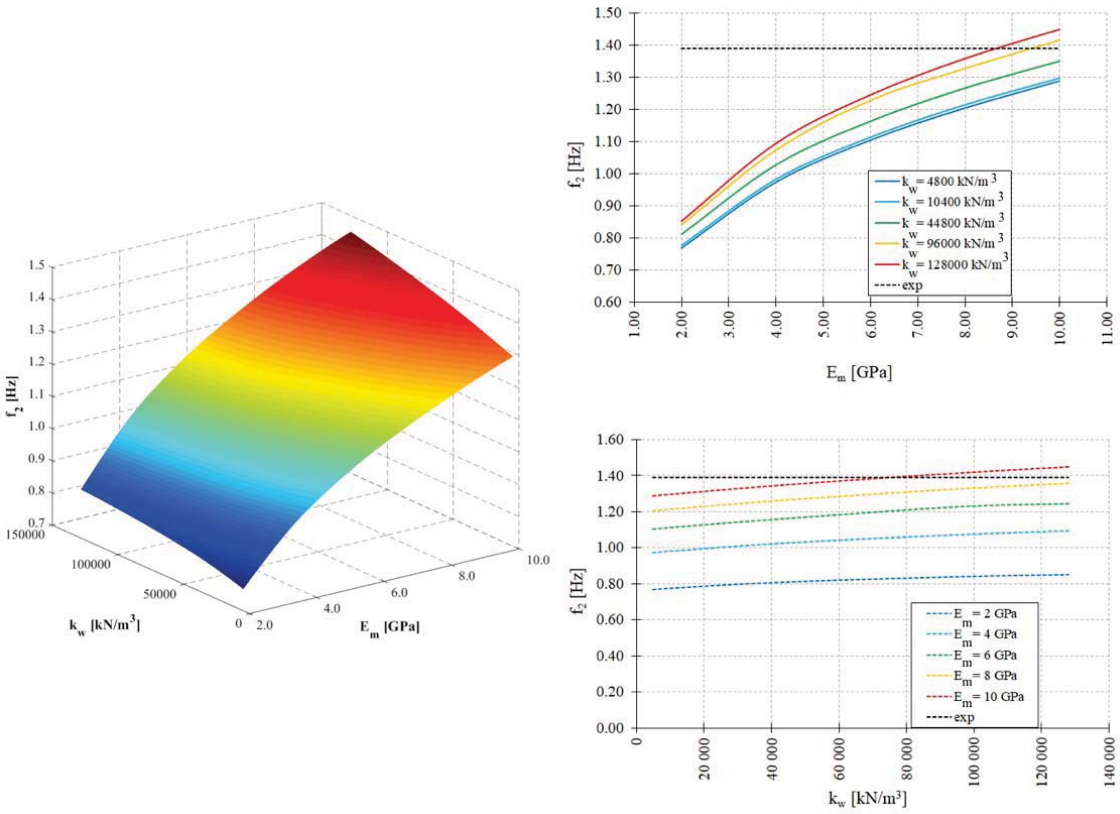

Figure 9: Model 2, second frequency as a function of Young's modulus E_m and soil stiffness k_w.

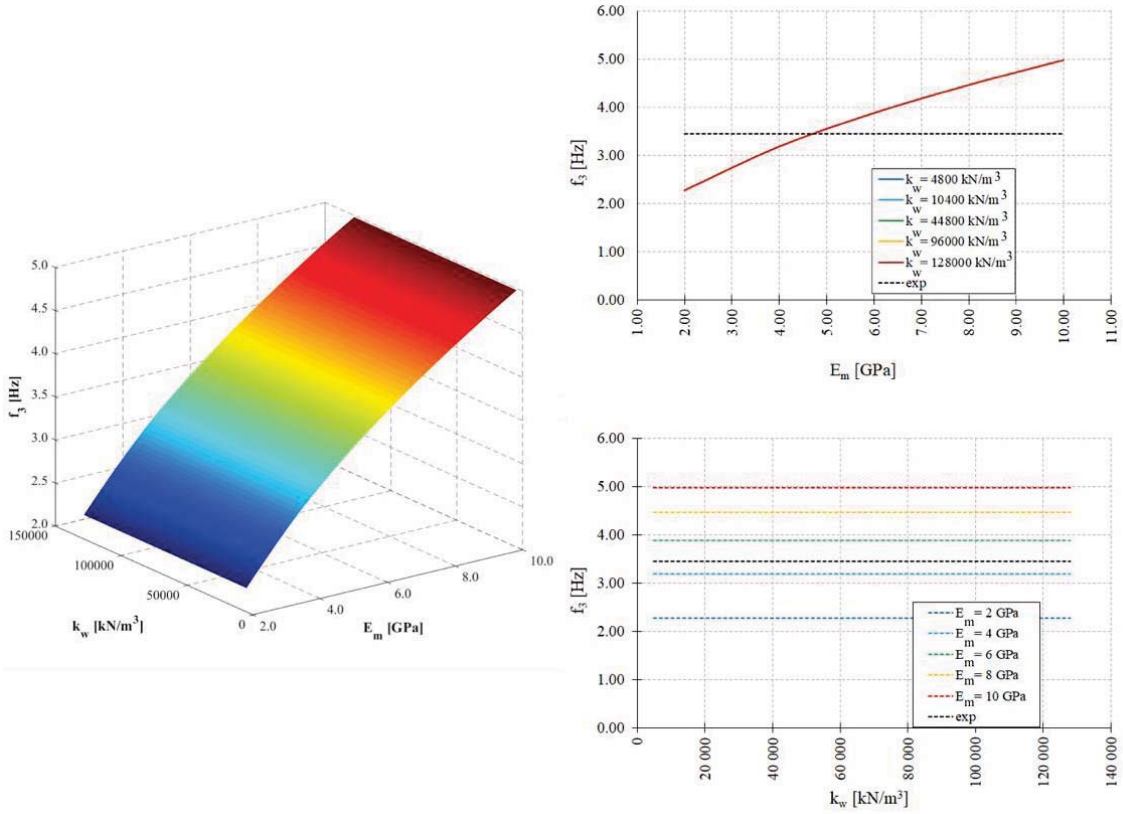

Figure 10: Model 2, third frequency as a function of Young's modulus E_m and soil stiffness k_w.

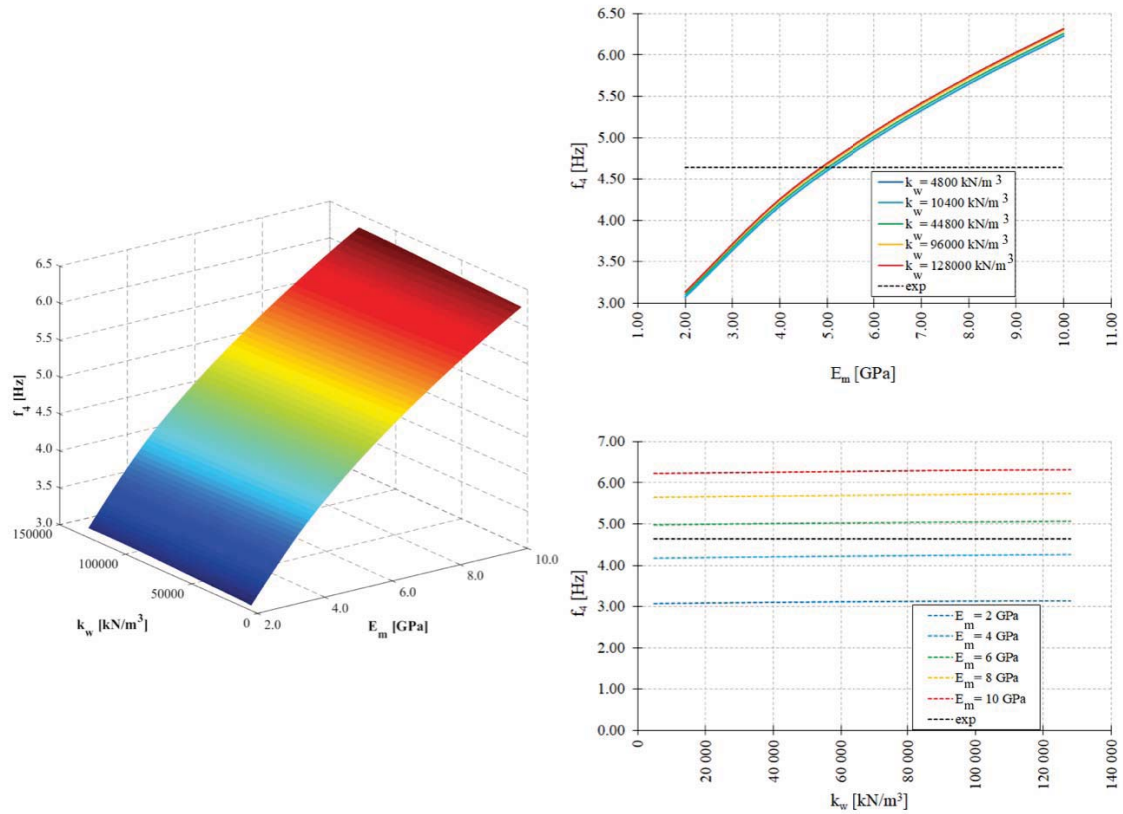

Figure 11: Model 2, fourth frequency as a function of Young's modulus E_m and soil stiffness k_w.

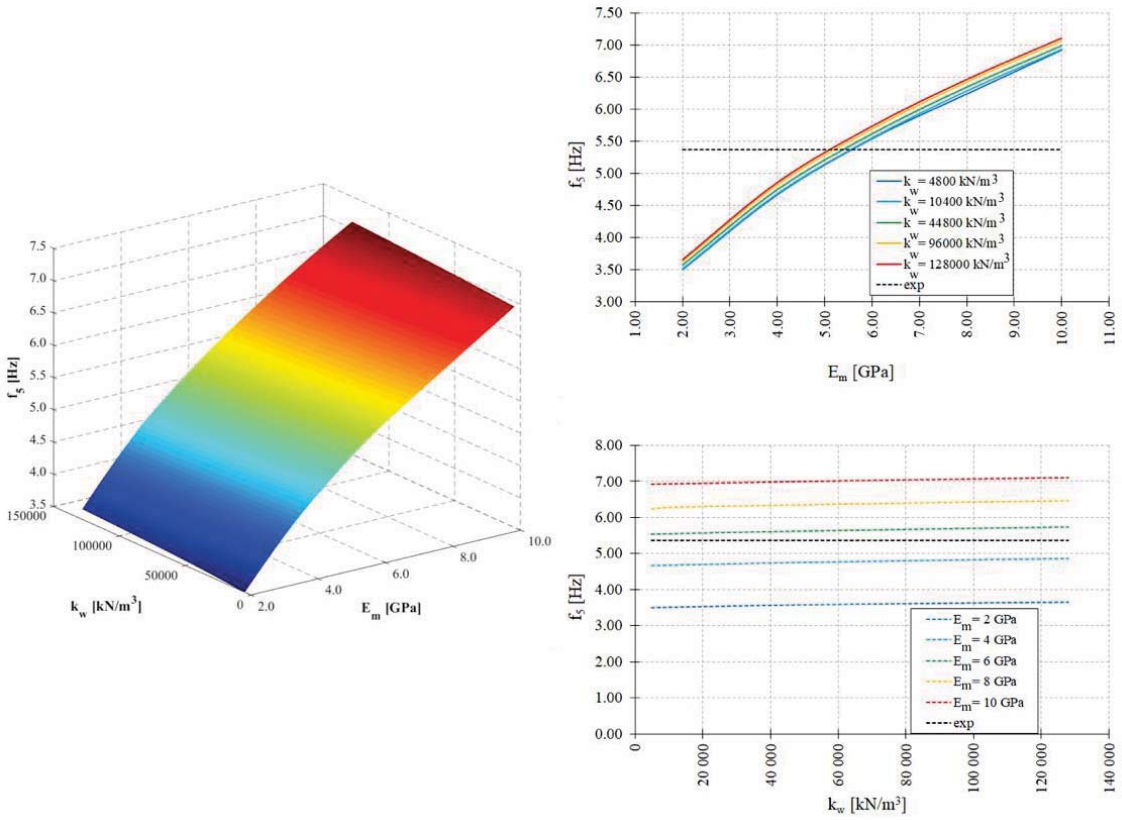

Figure 12: Model 2, fifth frequency as a function of Young's modulus E_m and soil stiffness k_w.

The results of the model updating procedure conducted on Model 2, for E_m [GPa] and k_w [kN/m^3] varying in the intervals given in (2), as in the case of Model 1, are the following

$$E_m^{opt} = 5.327 \text{ GPa}, \qquad k_w^{opt} = 1.28\ 10^5 \text{ kN/m}^3, \tag{4}$$

with k_w^{opt} coinciding with the right end of the interval in (2). The corresponding numerical frequencies and the relative errors with respect to the experimental frequencies are summarized in Table 3.

	Exp. freq. [Hz]	Num. freq. [Hz]	Relative error [%]
Mode 1	1.11	0.98	11.71
Mode 2	1.39	1.29	7.19
Mode 3	3.45	3.65	-5.80
Mode 4	4.64	4.64	0.0
Mode 5	5.37	5.71	-6.33

Table 3: The first five numerical frequencies of Model 2 corresponding to the optimal values in (4) with the relative errors with respect to the experimental values.

The errors in this case are still consistent, but lower (about one half) than those shown in Table 2 for Model 1.

Finally, if model updating is performed considering as unknown parameters E_m, k_w and the elastic constants k_{X1}, k_{X2} and k_Y of the lateral springs as well, for k_{X1}, k_{X2} and k_Y [N/m] varying in the interval [1.0 10^8, 7.0 10^{21}], then the optimal values are

$$E_m^{opt} = 4.53 \text{ GPa}, \quad k_w^{opt} = 0.69389\ 10^5 \text{ kN/m}^3, \quad k_{X1}^{opt} = k_{X2}^{opt} = k_Y^{opt} = 3.5\ 10^{21} \text{ N/m}. \tag{5}$$

The corresponding numerical frequencies and the relative errors with respect to the experimental frequencies are reported in Table 4.

	Exp. freq. [Hz]	Num. freq. [Hz]	Relative error [%]
Mode 1	1.11	1.13	-1.80
Mode 2	1.39	1.39	0.0
Mode 3	3.45	3.50	-1.45
Mode 4	4.64	4.97	-7.11
Mode 5	5.37	6.05	-12.66

Table 4: The first five numerical frequencies of Model 2 corresponding to the optimal values in (5) with the relative errors with respect to the experimental values.

For the sake of comparison, we recall the results obtained in [13] considering the tower clamped at the base and assuming that the horizontal displacements of the points adjacent to the church (magenta and red points in Figure 2) are prevented. The model updating conducted in [13] with E_m as the unknown parameter yielded the following optimal value

$$E_m^{opt} = 4.20 \text{ GPa}, \tag{6}$$

and the frequencies reported in Table 5.

	Exp. freq. [Hz]	Num. freq. [Hz]	Relative error [%]
Mode 1	1.11	1.18	-6.31
Mode 2	1.39	1.43	-2.88
Mode 3	3.45	3.37	-2.32
Mode 4	4.64	4.93	-6.25
Mode 5	5.37	6.00	-11.73

Table 5: The first five numerical frequencies of the tower clamped at the base with the horizontal displacements prevented [13] corresponding to the optimal value in (6) with the relative errors with respect to the experimental values.

Thus, a comparison of Table 4 to Table 5 shows that taking into account both the deformability of the adjacent constraints and the soil–structure interaction allows for appreciably fine-tuning the model and improving the simulation of the experimental results.

4 CONCLUSIONS

This paper is devoted to studying the effects of soil deformability and adjacent buildings on the dynamic behavior of masonry towers. The investigation relies on the use of some experimental results collected during a long-term dynamic monitoring campaign on the San Frediano bell tower in Lucca and an automated model updating procedure implemented in the NOSA-ITACA code.

The paper shows that soil stiffness can significantly affect the dynamic behavior of isolated towers, while in the case of towers connected to other buildings, the model's global stiffness is very sensitive to the kind of connection with the adjacent structures. The use of automated model updating procedures can help fine-tune the FE model, and enables estimating the stiffness of both the soil and the lateral constraints.

REFERENCES

[1] J.E. Mottershead, M.I. Friswell, Model updating in structural dynamics: a survey, *Journal of Sound and Vibration*, 167(2), 347-375, 1993.

[2] Á. Bautista-De Castro, L.J. Sánchez-Aparicio, L.F. Ramos, J. Sena-Cruz, D. González-Aguilera, Integrating geomatic approaches, Operational Modal Analysis, advanced numerical and updating methods to evaluate the current safety conditions of the historical Bôco Bridge, *Construction and Building Materials*, 158, 961-984, 2019.

[3] A. Cabboi, C. Gentile, A. Saisi, From continuous vibration monitoring to FEM-based damage assessment: application on a stone-masonry tower, *Construction and Building Materials*, 156, 252-265, 2017.

[4] R. Ferrari, D. Froio, E. Rizzi, C. Gentile, E.N. Chatzi, Model updating of a historic concrete bridge by sensitivity-and global optimization-based Latin Hypercube Sampling, *Engineering Structures*, 179, 139-160, 2019.

[5] M. Girardi, C. Padovani, D. Pellegrini, L. Robol, A model updating procedure to enhance structural analysis in the FE code NOSA-ITACA, *Journal of Performance of Constructed Facilities*, Vol. 33, Issue 4, 2019.

[6] M. Girardi, C. Padovani, D. Pellegrini, M. Porcelli, L. Robol, Finite element model updating for structural applications, *Journal of Computational and Applied Mathematics*, *370*, 112675, 2020.

[7] R. Lancellotta, D. Sabia, Identification technique for soil-structure analysis of the Ghirlandina tower, *International Journal of Architectural Heritage*, 9(4), 391-407, 2015.

[8] F. Lorenzoni, M.R. Valluzzi, M. Salvalaggio, A. Minello, C. Modena, Operational modal analysis for the characterization of ancient water towers in Pompei, *Procedia engineering*, 199, 3374-3379, 2017.

[9] M. Papadopoulos, R. Van Beeumen, S. François, G. Degrande, G. Lombaert, Computing the modal characteristics of structures considering soil-structure interaction effects, *Procedia engineering*, 199, 2414-2419, 2017.

[10] R.M. Azzara, A. De Falco, M. Girardi, D. Pellegrini, Ambient vibration recording on the Maddalena Bridge in Borgo a Mozzano (Italy): data analysis, *Annals of Geophysics*, 60 (4), S0441, 2017.

[11] G. Zani, P. Martinelli, A. Galli, C. Gentile, M. di Prisco, Seismic Assessment of a 14th-Century Stone Arch Bridge: Role of Soil–Structure Interaction, *Journal of Bridge Engineering*, 24(7), 05019008, 2019.

[12] G. Torelli, D. D'Ayala, M. Betti, G. Bartoli, Analytical and numerical seismic assessment of heritage masonry towers, *Bulletin of Earthquake Engineering*, 18(3), 969-1008, 2020.

[13] R.M. Azzara, G. De Roeck, M. Girardi, C. Padovani, D. Pellegrini, E. Reynders, Assessment of the dynamic behaviour of an ancient masonry tower in Lucca via ambient vibrations, in *Proceedings of the 10th international conference on the Analysis of Historical Constructions-SAHC 2016*, CRC Press, pp. 669-675, 2016.

[14] J.E. Bowles, Foundation analysis and design, McGraw-Hill, USA, 1996.

[15] www.nosaitaca.it/software

[16] M. Porcelli, V. Binante, M. Girardi, C. Padovani, G. Pasquinelli, A solution procedure for constrained eigenvalue problems and its application within the structural finite-element code NOSA-ITACA, *Calcolo*, *52*(2), 167-186, 2015.

[17] R. Brincker, C. Ventura, Introduction to Operational Modal analysis, Wiley, 2015.

[18] E. Reynders, K. Maes, G. Lombaert, G. De Roeck, Uncertainty quantification in operational modal analysis with stochastic subspace identification: Validation and applications, *Mech. Syst. Signal Process* 66-67:13-30, 2016.

[19] E. Reynders, M. Schevenels, G. De Roeck, MACEC 3.3. A Matlab toolbox for experimental and operational modal analysis. http://bwk.kuleuven.be/bwm/macec/, 2014.

[20] Circolare 21 gennaio 2019, n. 7 C.S.LL.PP. Istruzioni per l'applicazione dell'«Aggiornamento delle "Norme tecniche per le costruzioni"», D.M. 17 gennaio 2018.